Mecánica Computacional Vol. XXIV
A. Larreteguy (Editor)
Buenos Aires, Argentina, Noviembre 2005

NUMERICAL SIMULATION OF GROUNDWATER CONTAMINATION BY ETHANOL-AMENDED GASOLINE

Jonas Cordazzo, Clovis R. Maliska
Computational Fluid Dynamics Laboratory
Mechanical Engineering Department-UFSC
88040-900 - Florianópolis-SC-Brazil (maliska@sinmec.ufsc.br)

and

Henry X. Corseuil
Department of Environmental Engineering-UFSC
88040-900 - Florianópolis-SC-Brazil

Key words: water contamination, groundwater, ground water simulation, ethanol-amended gasoline

Abstract. *This paper presents a numerical procedure for simulating the dispersion of ethanol-amended gasoline in ground water flows. In this problem the degree of influence of the ethanol in the biodegradation of the BTEX compounds is not known, since the common models does not include the presence of ethanol. The transport equation includes the dispersion, advection, sorption and biodegradation of the compounds BTEX and ethanol carried by the flow of water modeled using the Darcy's equation for porous media flow. The mathematical model is solved using the finite volume method with a first-order decay mode for the biodegradation. It is assumed that the hydrophobic organic compounds solubility in the aqueous-phase increases log-linearly with the presence of ethanol, in a phenomenon called the "co-solvency effect". The sorption phenomenon (retard of the plume) is modeled using linear equilibrium isotherm. To evaluate the model and demonstrate its potentialities, it is solved some groundwater contamination problems with ethanol-amended gasoline.*

1. INTRODUCTION

Environmental protection agencies around the world have demonstrated that the soil has been frequently contaminated by spills during explotation, refinement, transport and operations of petroleum and its derivates. Gasoline, the most important petroleum derivate, offers high potential risk of contamination because its BTEX compounds (benzene, toluene, ethyl-benzene and xylems) are released when the gasoline is in contact with the groundwater. These are dangerous substances because they affect the central nervous system and may cause several serious diseases. In Brazil this problem is crucial since the fuel storage tanks were made in 70's and their life duration is estimated in about 25 years. Consequently, it is expected an increasing number of spills in Brazilian's gas station tanks. Additionally, the refineries and processing plants offers increased risk of larger spills which may put in danger larger areas.

Several models that provide analytical and numerical simulations for the groundwater contamination can be found in the literature. The "Bioscreen" software[1], for example, is one of the available tools for simulation of groundwater contamination. It includes three different models: solute transport without decay, solute transport with first order decay biodegradation and solute transport, with biodegradation modeled with instantaneous biodegradation reaction. It is based on the Domenico's analytical model[2] that assumes an infinite vertical source of constant concentration.

Rifai *et al*.[3], on the other hand, developed the "Bioplume III", that is a finite-difference model for the simulation of natural attenuation of organic contaminant in groundwater, including the advection, dispersion, sorption and biodegradation processes. This numerical tool is based on the Method of Characteristics (MOC), which includes the water flow equations with the solute transport equations[4].

In Brazil, however, the commercial gasoline is amended with 24 % of alcohol (ethanol) and this causes a different behavior of the plume dispersion[5] compared with the plume without ethanol. The plume of the BTEX compounds, as expected, contaminates a larger region, since its biodegradation starts only after the ethanol is biodegraded. Therefore, the available models do not apply to these situations. This paper is devoted for the development of numerical model for the prediction of the dispersion of contaminants when ethanol-amended gasoline is considered. Tests problems are presented for evaluating the model and show the influence of the ethanol in the concentration of the BTEX compounds.

2. PHYSICAL CONSIDERATIONS

Gasoline is a mixture of volatile hydrocarbons, which include the benzene, toluene, ethyl-benzene and xylems elements (called BTEX group). BTEX compounds are among the most water-soluble, mobile and potentially harmful hydrocarbons found in gasoline.

2.1. Influence of ethanol in the BTEX biodegradation.

Kinetics correlations have been developed to estimate the biotransformation of organic contaminants. A simple alternative for modeling the biodegradation rate is the use of a first order decay, given by

$$\frac{dC}{dt} = -\delta\lambda C \tag{1}$$

where C is the concentration and λ is the first-order degradation coefficient. The coefficient δ ranges from 0 to 1, depending on the alcohol concentration. The physical explanation for this

coefficient is now given. Santos[6] observed in his experiments that microorganisms prefer to degrade ethanol, retarding the BTEX compounds biodegradation. This phenomenon is represented in Fig. 1 for benzene, as an example, where the pure contaminant (no alcohol mixed) was all consumed in less than 4 days, while there is no significant biodegradation in 12 days in the mixture with 300 mg/L of ethanol.

The most probable cause for no degradation of BTEX compounds in presence of ethanol is the fact that the ethanol is a simpler substrate than benzene, toluene, ethyl benzene and xylems and, therefore, is easier to biodegrade by microorganisms.

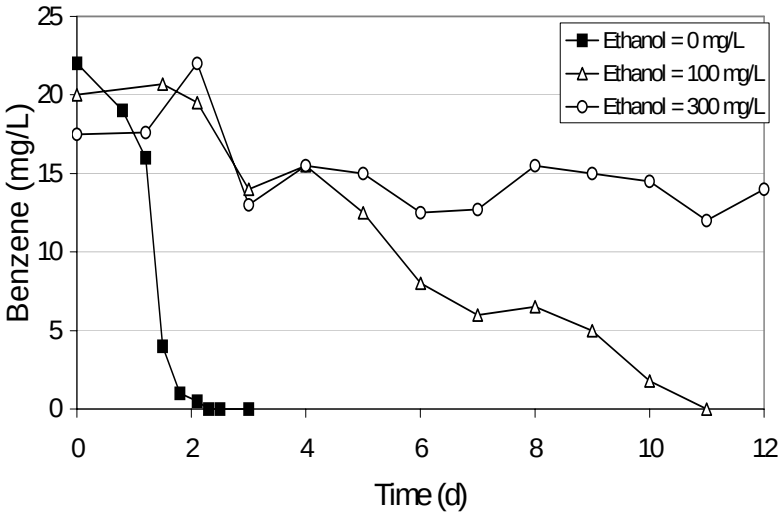

Fig. 1. Effects of ethanol concentrations in the benzene aerobic biodegradation, Santos[6]

2.2. The co-solvency effect of ethanol in the gasoline.

The effective co-solvency of an organic compound in the gasoline can be estimated from the aqueous solubility of the pure component and its mole fraction in the gasoline. The solubility in the gasoline increases if the compound has oxygen, such as alcohols and ethers. When the gasoline is in contact with the water, the alcohol existent in this gasoline, due to be fully miscible in water, will migrate for the groundwater[7]. Therefore, high concentrations of ethanol in water facilitate the transfer of the BTEX existing in the gasoline to the aqueous-phase, increasing the aromatic hydrocarbon solubility in the groundwater, in a process called “co-solvency effect”.

A simple mathematical model for predicting the possible increase of the contaminant solubility in presence of ethanol in groundwater assumes, in a mixture of binary solvents, that the solubility of hydrophobic compounds in water (BTEX, for example) increases log-linearly with the volume fraction of fully miscible organic solvents. This relationship can be expressed, as proposed by Yalkowsky and Roseman[8], by

$$\log(S_m) = \log(S_w) + f_c \bar{\beta} \tag{2}$$

where S_w and S_m are the solubility in water and in the water-co-solvent mixture, respectively, f_c is the volume fraction of the co-solvent (ethanol, for example) in the aqueous phase, and $\bar{\beta}$ is a measure of the relative ability of the co-solvent to increase the solubility of hydrophobic organic compounds (co-solvency power). For the mixture of BTEX and ethanol, Corseuil and Fernandez[7] recommend the following expression

$$\overline{\beta} = 1.02 \log(K_{ow}) - 1.52 \tag{3}$$

where K_{ow} is the octanol-water partitioning coefficient that represents the compounds hydrophobicity[9]. For the BTEX compounds, the log (K_{ow}) ranges from 2 to 3, according to Howard[10]. Laboratory experiments have demonstrated that the total mass of BTEX compounds increases in about 10 to 30 % of ethanol fraction in the water[7].

2.3.The Sorption effect – the interaction of contaminant with the soil

The fate of hydrophobic organic pollutants in a natural water system is also dependent upon the sorption behavior. The sorption effect is determined experimentally by measuring the contaminant in a particular sediment, soil or rocks. The Freundlich's isotherm is the non-linear model largely used[11], and can be written as

$$S = K_d C^b \tag{4}$$

where K_d is the partition coefficient and b is a coefficient obtained experimentally. If b = 1, Eq.(4) is known as linear isotherm. The linear isotherm is appropriate for cases where the sorption potential increases uniformly with the concentration. This model has been shown suitable in cases of very low solute concentrations and for solids of low sorption potential[11].

3. MATHEMATICAL FORMULATION

The mathematical model used in this work involves the solution of Darcy's equation in the porous media, the solute transport equations for the BTEX and ethanol components. Darcy's Law states that the velocity vector $\vec{V}'$ can be given by

$$\vec{V}' = -\frac{k}{\mu} \nabla P \tag{5}$$

where k is the absolute permeability (scalar or anisotropic tensor), μ is the groundwater viscosity and P the pressure.

Considering the physical phenomena presented in the previous section, it is easy to show that the transient transport equation of a specie, involving the decay, adsorption, and a mass source of contaminant by pumping/suction is given by

$$\frac{\partial(\rho C)}{\partial t} = \frac{1}{R}\left[\frac{\partial}{\partial x_i}\left(\rho D_{ij}\frac{\partial C}{\partial x_j}\right) - \frac{\partial(\rho C V_i)}{\partial x_i}\right] - \lambda\delta\rho C + \frac{W\rho C}{n\Delta x\Delta y\Delta z} \tag{6}$$

where ρ is fluid density, n the porosity, V_i the average interstitial velocity in the direction i, obtained by dividing the Darcy's velocity (average velocity in the volume) by the porosity n, C the concentration of transported solute, D_{ij} the second order tensor called mechanical dispersion, λ the first order decay coefficients of contaminant in the solution, W the volumetric source, which assumes negative sign in cases of suction. The factor, R, has the effect of retarding the adsorbed species in relation to the groundwater advective velocity, and it is given by

$$R = 1 + \frac{\rho_b}{n} K_d \tag{7}$$

where ρ_b is the bulk specific mass of the porous medium. In equation (6) the experimental coefficient of sorption *b*, Eq. (4), was assumed equal to 1.0, meaning that the substrate decays in the same manner in the solution and in the adsorbed phase. Details and a complete derivation of this equation can be found in Cordazzo and Maliska[12].

4. NUMERICAL FORMULATION

The task of a numerical technique is to transform a partial differential equation, like Eq. (6), in a system of *n* linear algebraic equations with *n* unknowns, one for each node. This procedure is realized here using the finite volume method. The resulting discrete equations obeys the conservation principle at discrete level. The discretized equations are obtained by integrating the conservative transport equation in the elemental control volume shown in Fig. 2.

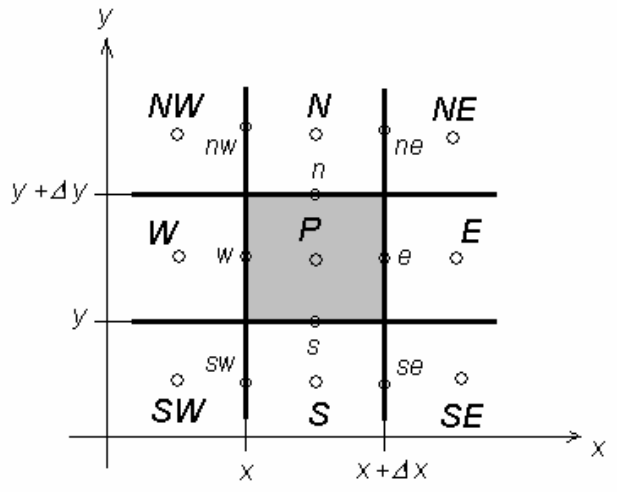

Fig. 2. Elementary control volume and its neighbors

The domain is discretized using Cartesian grids with constant thickness, even though different grid types can be used using the same physical, mathematical and numerical modeling presented herein.

4.1 Discretization of the advection/diffusion transport equation

Therefore, integrating Eq. (6) in time and space, including the *z* direction between 0 and ΔH (the domain thickness),

$$\int_t^{t+\Delta t}\int_w^e\int_s^n\int_0^{\Delta H}\left\{\frac{1}{R}\left[\frac{\partial}{\partial x_i}\left(\rho D_{ij}\frac{\partial C}{\partial x_j}\right)-\frac{\partial(\rho C V_i)}{\partial x_i}\right]-\lambda\rho\delta C+\frac{W\rho C}{n\Delta x\Delta y\Delta H}\right\}dzdydxdt=\int_t^{t+\Delta t}\int_w^e\int_s^n\int_0^{\Delta H}\left(\frac{\partial(\rho C)}{\partial t}\right)dzdydxdt \tag{8}$$

resulting in

$$\left[\left(\rho\frac{D_{xx}}{R}\frac{\partial C}{\partial x}+\rho\frac{D_{xy}}{R}\frac{\partial C}{\partial y}\right)\Big|_e-\left(\rho\frac{D_{xx}}{R}\frac{\partial C}{\partial x}+\rho\frac{D_{xy}}{R}\frac{\partial C}{\partial y}\right)\Big|_w-\rho\frac{u}{R}\Big|_e C_e+\rho\frac{u}{R}\Big|_w C_w\right]\Delta H\Delta y\Delta t+$$
$$\left[\left(\rho\frac{D_{yx}}{R}\frac{\partial C}{\partial x}+\rho\frac{D_{yy}}{R}\frac{\partial C}{\partial y}\right)\Big|_n-\left(\rho\frac{D_{yx}}{R}\frac{\partial C}{\partial x}+\rho\frac{D_{yy}}{R}\frac{\partial C}{\partial y}\right)\Big|_s-\rho\frac{v}{R}\Big|_n C_n+\rho\frac{v}{R}\Big|_s C_s\right]\Delta H\Delta x\Delta t$$
$$-\left(\lambda\delta\rho-\frac{W\rho}{n\Delta x\Delta y\Delta H}\right)C_P\Delta x\Delta y\Delta H\Delta t=\left(\rho C_P-\rho^o C_P{}^o\right)\Delta x\Delta y\Delta H \tag{9}$$

where the superscript (o) indicates that the variable is evaluated at the previous time level.

It can be seen in Eq. (9) that the derivatives and the values of the concentration are required at the interfaces of the control volume. The cross-derivatives terms are evaluated using CDS approximations, while the remaining diffusive and advective terms uses the WUDS (*Weighted Upstream Differencing Scheme*) procedure proposed by Raithby and Torrance[13]. Therefore,

$$C_e=\left(\frac{1}{2}+\alpha_e\right)C_P+\left(\frac{1}{2}-\alpha_e\right)C_E \tag{10}$$

and,

$$\frac{\partial C}{\partial x}\Big|_e=\beta_e\left(\frac{C_E-C_P}{\Delta x_e}\right) \tag{11}$$

where α and β are coefficients depending on the Peclet number, *Pe*. They are defined by

$$\alpha_e=\frac{1}{2}-\frac{e^{\frac{Pe}{2}}-1}{e^{Pe}-1} \tag{12}$$

$$\beta_e=Pe\frac{e^{\frac{Pe}{2}}}{e^{Pe}-1} \tag{13}$$

The Peclet number, *Pe*, is defined as the ratio of advective and diffusive mass fluxes, by

$$Pe=\frac{V\Delta L}{D} \tag{14}$$

where V is the interstitial velocity component in a direction (u or v), ΔL is the volume dimension in this direction, i. e. Δx or Δy, respectively, and D is the dispersion coefficient.

Another important characteristic of the model advanced in this paper is that it can handle domains with different permeabilities. Hence, it is necessary to have a special treatment for the cross-derivatives terms. As already stated, in a situation of uniform permeability (homogeneous media), the cross-derivative terms are discretizated by central differences, but in the heterogeneous cases this approximation is not recommended. A good option would be to have an interpolation function that weights the cross derivative approximation as a function of the

permeability. For example, the cross derivative approximation in the face *e* of Fig. 2 could have the form

$$D_{xy}\left.\frac{\partial C}{\partial y}\right|_e = \bar{\alpha}_{xy}\frac{C_P + C_E - C_{SE} - C_S}{4\Delta y} + \bar{\beta}_{xy}\frac{C_{NE} + C_N - C_P - C_E}{4\Delta y} \tag{15}$$

where $\bar{\alpha}_{xy}$ and $\bar{\beta}_{xy}$ are factors that have the role of representing physically consistent the value of the dispersion tensor component D_{xy} for each face. Details about the determination of the dispersion tensor components can be found in Bear[14]. Thus, if in Fig. 2, for example, the permeability in volumes *S* and/or *SE* are equal to zero, Eq. (15) should be written as

$$D_{xy}\left.\frac{\partial C}{\partial y}\right|_e = \left(\frac{2D_{xy}\big|_e D_{xy}\big|_{ne}}{D_{xy}\big|_e + D_{xy}\big|_{ne}}\right)\left(\frac{C_{NE} + C_N - C_P - C_E}{2\Delta y}\right) \tag{16}$$

when, $\bar{\alpha}_{xy}$ and $\bar{\beta}_{xy}$ are given by

$$\bar{\alpha}_{xy} = 0$$

and

$$\bar{\beta}_{xy} = \left.\frac{4D_{xy}\big|_e D_{xy}\big|_{ne}}{D_{xy}\big|_e + D_{xy}\big|_{ne}}\right|_e \tag{17}$$

Cordazzo[15] proposed the evaluation of $\bar{\alpha}_{xy}$ and $\bar{\beta}_{xy}$ by

$$\bar{\alpha}_{xy}\big|_e = \frac{4\left|D_{xy_{se}} D_{xy_e}\right|}{\left|D_{xy_{se}}\right| + \left|D_{xy_e}\right|}\left(1 - \frac{\left|D_{xy_{ne}}\right|}{\left|D_{xy_e}\right| + \left|D_{xy_{ne}}\right|}\right)\frac{D_{xy_e}}{\left|D_{xy_e}\right|} \tag{18}$$

$$\bar{\beta}_{xy}\big|_e = \frac{4\left|D_{xy_{ne}} D_{xy_e}\right|}{\left|D_{xy_{ne}}\right| + \left|D_{xy_e}\right|}\left(1 - \frac{\left|D_{xy_{se}}\right|}{\left|D_{xy_e}\right| + \left|D_{xy_{se}}\right|}\right)\frac{D_{xy_e}}{\left|D_{xy_e}\right|} \tag{19}$$

where the values between the | | are absolute values.

As a demonstration of the behavior of these factors, consider in the Fig. 2 that $D_{xy|ne} = D_{xy|e}$. The variation of $\bar{\alpha}_{xy}$ and $\bar{\beta}_{xy}$ with the dispersion coefficient in the interface "*se*" is analyzed in the Fig. 3. One can note that when the dispersion at the interface "*se*" increases, the factor $\bar{\alpha}_{xy}$ tends to the value $2D_{xy}$ and the factor $\bar{\beta}_{xy}$ tends to zero. This characteristic is obvious since the derivative at the face "*e*" should be first order approximated. On the other hand, when the domain is homogeneous, the factors $\bar{\alpha}_{xy}$ and $\bar{\beta}_{xy}$ are equal to D_{xy}, what recovers the approximation of centered differences (second order approximation). On the contrary, when D_{xy} in the face "*se*" decreases, the factor $\bar{\alpha}_{xy}$ tends to zero and the factor $\bar{\beta}_{xy}$ tends to $2D_{xy}$.

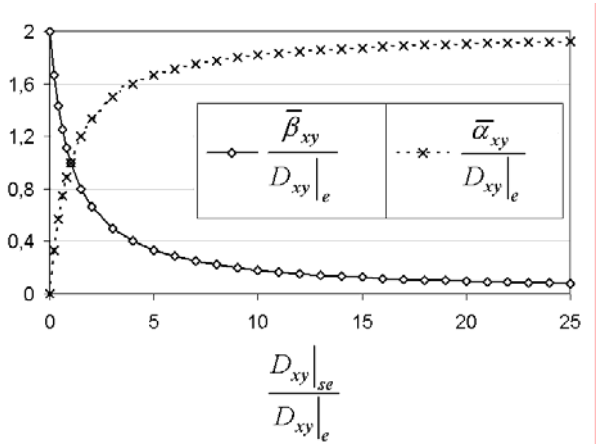

Fig. 3. Variation of factors $\overline{\alpha}_{xy}$ and $\overline{\beta}_{xy}$ in function of dispersion D_{xy} at the interface "*se*" of Fig. 2, assuming that interfaces "*ne*" and "*e*" have the same transversal dispersion.

Considering an equally-spaced grid and a fully implicit formulation, Eq. (9) reads

$$\begin{aligned}
&\left\{\left[\rho\frac{D_{xx}}{R}\Big|_e\beta_e\left(\frac{C_E-C_P}{\Delta x}\right)+\rho\frac{\overline{\alpha}_{xy}}{R}\Big|_e\left(\frac{C_P+C_E-C_S-C_{SE}}{4\Delta y}\right)+\rho\frac{\overline{\beta}_{xy}}{R}\Big|_e\left(\frac{C_{NE}+C_N-C_P-C_E}{4\Delta y}\right)\right]+\right.\\
&\quad-\left[\rho\frac{D_{xx}}{R}\Big|_w\beta_w\left(\frac{C_P-C_W}{\Delta x}\right)+\rho\frac{\overline{\alpha}_{xy}}{R}\Big|_w\left(\frac{C_P+C_W-C_S-C_{SW}}{4\Delta y}\right)+\rho\frac{\overline{\beta}_{xy}}{R}\Big|_w\left(\frac{C_{NW}+C_N-C_P-C_W}{4\Delta y}\right)\right]+\\
&\quad\left.-\rho\frac{u}{R}\Big|_e\left[\left(\frac{1}{2}+\alpha_e\right)C_P+\left(\frac{1}{2}-\alpha_e\right)C_E\right]+\rho\frac{u}{R}\Big|_w\left[\left(\frac{1}{2}+\alpha_w\right)C_W+\left(\frac{1}{2}-\alpha_w\right)C_P\right]\right\}\Delta y\Delta H+\\
&+\left\{\left[\rho\frac{\overline{\alpha}_{yx}}{R}\Big|_n\left(\frac{C_P+C_N-C_W-C_{NW}}{4\Delta x}\right)+\rho\frac{\overline{\beta}_{yx}}{R}\Big|_n\left(\frac{C_{NE}+C_E-C_P-C_N}{4\Delta x}\right)+\rho\frac{D_{yy}}{R}\Big|_n\beta_n\left(\frac{C_N-C_P}{\Delta y}\right)\right]+\right.\\
&\quad-\left[\rho\frac{\overline{\alpha}_{yx}}{R}\Big|_s\left(\frac{C_P+C_S-C_W-C_{SW}}{4\Delta x}\right)+\rho\frac{\overline{\beta}_{yx}}{R}\Big|_s\left(\frac{C_{SE}+C_E-C_P-C_S}{4\Delta x}\right)+\rho\frac{D_{yy}}{R}\Big|_s\beta_s\left(\frac{C_P-C_S}{\Delta y}\right)\right]+\\
&\quad\left.-\rho\frac{v}{R}\Big|_n\left[\left(\frac{1}{2}+\alpha_n\right)C_P+\left(\frac{1}{2}-\alpha_n\right)C_N\right]+\rho\frac{v}{R}\Big|_s\left[\left(\frac{1}{2}+\alpha_s\right)C_S+\left(\frac{1}{2}-\alpha_s\right)C_P\right]\right\}\Delta x.\Delta H+\\
&-\left(\lambda\delta\rho-\frac{W\rho}{n\Delta x\Delta y\Delta H}\right)C_P\Delta x\Delta y\Delta H=\frac{\left(\rho C_P-\rho^o C_P{}^o\right)}{\Delta t}\Delta x\Delta y\Delta H
\end{aligned}\tag{20}$$

Therefore, the general equation for the concentration, in a compact form, is given by

$$A_pC_P=A_eC_E+A_wC_W+A_nC_N+A_sC_S+A_{ne}C_{NE}+A_{se}C_{SE}+A_{nw}C_{NW}+A_{sw}C_{SW}+B \tag{21}$$

where A_p is the central coefficient, A_i are the connecting coefficients and B the independent term.

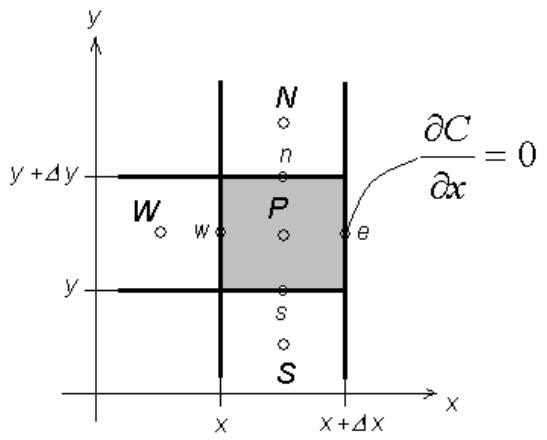

Fig. 4. Boundary control volume with zero derivative boundary condition

Now, the procedure for obtaining the discrete equations for the boundary volumes is presented. As example, the volume of Fig. 4 subject to a boundary condition of zero derivative of concentration in the face *e* is analyzed. Eq. (9), in this case, can be rewritten as

$$\left[\left(\rho\frac{D_{xy}}{R}\frac{\partial C}{\partial y}\right)\Big|_e-\left(\rho\frac{D_{xx}}{R}\frac{\partial C}{\partial x}+\rho\frac{D_{xy}}{R}\frac{\partial C}{\partial y}\right)\Big|_w-\rho\frac{u}{R}\Big|_e C_e+\rho\frac{u}{R}\Big|_w C_w\right]\Delta y\Delta H\Delta t+$$
$$+\left[\left(\rho\frac{D_{yx}}{R}\frac{\partial C}{\partial x}+\rho\frac{D_{yy}}{R}\frac{\partial C}{\partial y}\right)\Big|_n-\left(\rho\frac{D_{yx}}{R}\frac{\partial C}{\partial x}+\rho\frac{D_{yy}}{R}\frac{\partial C}{\partial y}\right)\Big|_s-\rho\frac{v}{R}\Big|_n C_n+\rho\frac{v}{R}\Big|_s C_s\right]\Delta x\Delta H\Delta t+$$
$$-\left(\lambda\delta\rho-\frac{W\rho}{n\Delta x\Delta y\Delta H}\right)C_P\Delta x\Delta y\Delta H\Delta t=\left(\rho C_P-\rho^o C_P{}^o\right)\Delta x\Delta y\Delta H \qquad (22)$$

After collecting terms, the concentration equation for the volume *P*, shown in the Fig. 4 is given by

$$A_pC_P=A_wC_W+A_nC_N+A_sC_S+A_{nw}C_{NW}+A_{sw}C_{SW}+B \qquad (23)$$

This boundary condition is called “local parabolic boundary condition”. For the volumes representing the contamination points of the groundwater, a prescribed and maximum value of concentration can be used, according to Raoult’s Law. Therefore, the coefficients for these volumes are given by

$$A_p=1$$
$$A_e=A_w=A_n=A_s=A_{nw}=A_{sw}=A_{se}=A_{ne}=0$$
$$B=\text{Prescribed Concentration Value}$$

It is clear that one does not need to obtain the approximated equation using the mass balance for these volumes, since the concentration is prescribed. One can use the mass balance to determine the dissolved mass. Thus, the dissolved mass, obtained integrating the equation (6) in the time and in the elemental control volume of Fig. 2, is given by

$$m_{dissolv.} = -\left\{ \frac{1}{R}\left[\left(D_{xx}\frac{\Delta C}{\Delta x} + D_{xy}\frac{\Delta C}{\Delta y} - uC \right)_e - \left(D_{xx}\frac{\Delta C}{\Delta x} + D_{xy}\frac{\Delta C}{\Delta y} - uC \right)_w \right] \Delta t \Delta y \Delta H n + \right.$$
$$\left. + \frac{1}{R}\left[\left(D_{yx}\frac{\Delta C}{\Delta x} + D_{yy}\frac{\Delta C}{\Delta y} - vC \right)_n - \left(D_{yx}\frac{\Delta C}{\Delta x} + D_{yy}\frac{\Delta C}{\Delta y} - vC \right)_s \right] \Delta t \Delta x \Delta H n - \lambda \delta \Delta x \Delta y \Delta H n C \Delta t \right\} \quad (24)$$

where the negative sign is required according to the definition used for the dissolved mass.

For a finite contamination source there will be a time where no more mass is available to sustain the prescribed concentration, and the concentration at the source should decrease in time, as expected. This condition can be easily implemented in the computational program, subtracting the dissolved mass ($m_{dissolv.}$) of the contamination source in each step time Δt. Fig. 5 illustrates the situation where there are two contamination sources in the groundwater. The procedure is analogous for a situation with more sources. It can be seen that the two sources acts independently while the plume does not reach the downstream source. That is mass is dissolved in both places, as shown in Fig. 5*(a)*. However, when the concentration of the volume containing the downstream source recovers its maximum value, by influence of the contamination of the upstream source, according to Raoult's Law, the downstream source ceases to dissolve mass, as we can see in the Figure 5 *(b)*, where the stored mass level, symbolized by the level of the vertical tubes, does not change. When the upstream source exhausts, the other source starts to contaminate again, Fig. 5*(c)*, until its mass finishes, Fig. 5*(d)*, when the residual contamination will be only transported and fully biodegraded.

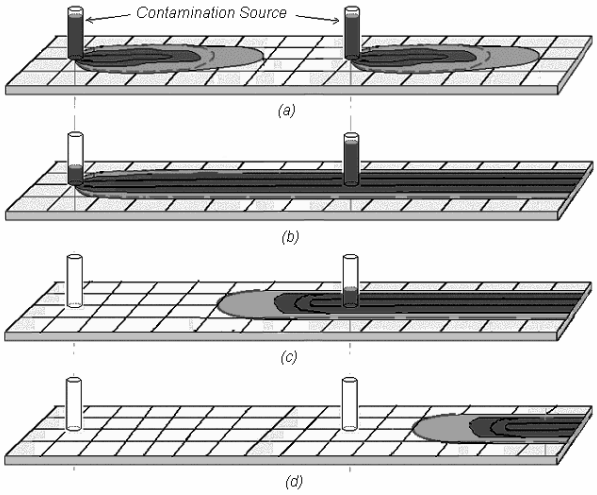

Fig. 5 – Aquifer exposed to two contamination sources: *(a)* beginning of the contamination, where the sources do not interfere themselves; *(b)* the upstream contamination source interferes in the other source, which does not dissolve more mass by Raoult's Law; *(c)* the upstream source becomes exhausted, permitting that the downstream source contaminates again; *(d)* the two sources became exhausted, and the residual contamination is only transported and biodegraded in the aquifer.

4.2 Discretization of the momentum equation

The governing equations for the flow in the porous media are given by the Darcy's equation,

$$u = \frac{u'}{n} = -\frac{k}{n\mu}\frac{\partial P}{\partial x}$$
$$v = \frac{v'}{n} = -\frac{k}{n\mu}\frac{\partial P}{\partial y} \tag{25}$$

where k is the permeability, μ is the groundwater viscosity and P the pressure.

Using Fig. 6, noting that the velocities are staggered related to pressure, and taking into account the heterogeneity of the medium using the harmonic averaging for the absolute permeability, Eq. (25), for the u-component at the east face, can be approximated by

$$u_e = \frac{u_e'}{n} = -\frac{1}{n\mu}\frac{2k_E k_P}{(k_E + k_P)}\frac{(P_E - P_P)}{\Delta x_e} \tag{26}$$

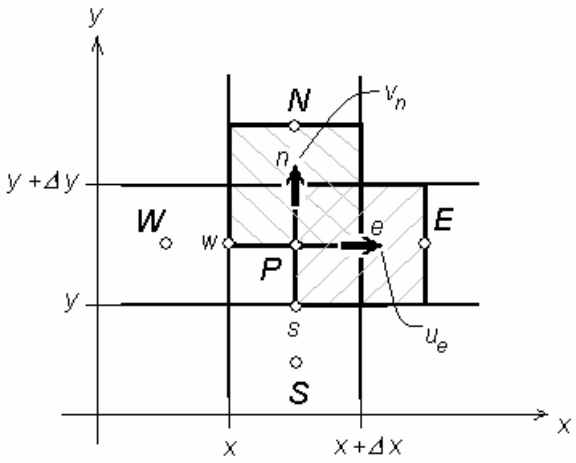

Fig. 6. Control volume for the pressure *P* and velocities *u* and *v*

Replacing the equations of u_e, u_w, v_n and v_s in the mass conservation equation for porous media[16],

$$\frac{\partial}{\partial t}(\rho n) + \frac{\partial(\rho u')}{\partial x} + \frac{\partial(\rho v')}{\partial y} = 0 \tag{27}$$

we obtain the general equation for the pressure, given by

$$A_P P_P = A_e P_E + A_w P_W + A_n P_N + A_s P_S + B \tag{28}$$

Solving for the pressure field, the velocities can be obtained from Eqs. (25). For the boundary volumes, the procedure to obtain the pressure equation was proposed by Maliska[17] for

boundary-fitted coordinates. It consists in just applying the mass conservation equation for these volumes, taking in account the boundary condition in that boundary. This procedure satisfies the balance for the boundary volumes and do not increase the number of equations of the linear system[18], a happens if fictitious boundary nodes are used.

5. RESULTS

In order to validate the model and to demonstrate its applicability, this section presents results for some key test problems.

5.1. Simulation of a two-dimensional problem

The first case analyzed is depicted in Fig. 7. This problem, involving first order decay, constant horizontal velocity and retard has analytical solution given by Sudicky[19].

The comparison between the analytical solution and the numerical solution using a grid with 30 x 60 volumes and time step of 1.8 s is shown in the Fig. 8. It can be seen that the numerical results are in good agreement with the analytical ones. In order to perform this comparison, the velocity field was assumed one dimensional with constant *u*-velocity. The nonzero components of dispersion tensor D_{ij}, neglecting the molecular diffusion, are given by Bear[14]:

$$D_{xx} = \alpha_L u \qquad \text{and} \qquad D_{yy} = \alpha_T u \tag{29}$$

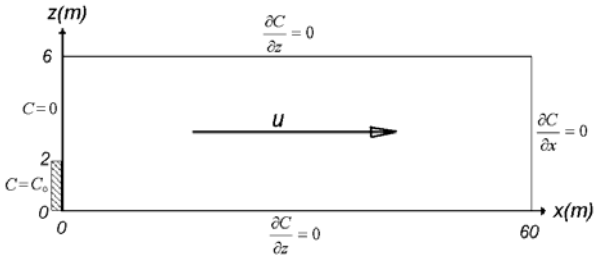

Fig. 7. Domain and boundary conditions of the two dimensional problem analyzed, with *u* = 0,09 m/d, α_L = 0,6 m, α_T = 0,005 m, *R* = 1,2 and λ = 0,007 day^{-1}

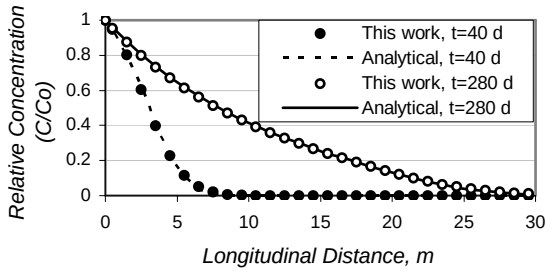

(a)

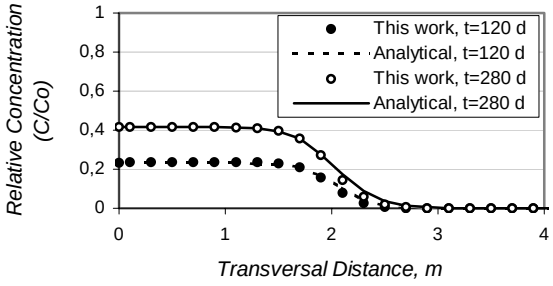

(b)

Fig. 8. Comparison between the numerical and analytical solution for the *(a)* longitudinal (z = 0) and *(b)* transversal (x = 10 m) concentration profile

5.2. Simulation of the five-spot problem

In this problem the flow in a porous media considering the advection and diffusion of a specie is considered and compared with experimental results. The problem chosen is the well-known 5-spot problem, where due to the well distribution, the boundaries of the domain result impermeable. A flow of water in steady-state exists between the injection and production well when, suddenly, it is inject in the injection well a tracer with specified concentration.

I

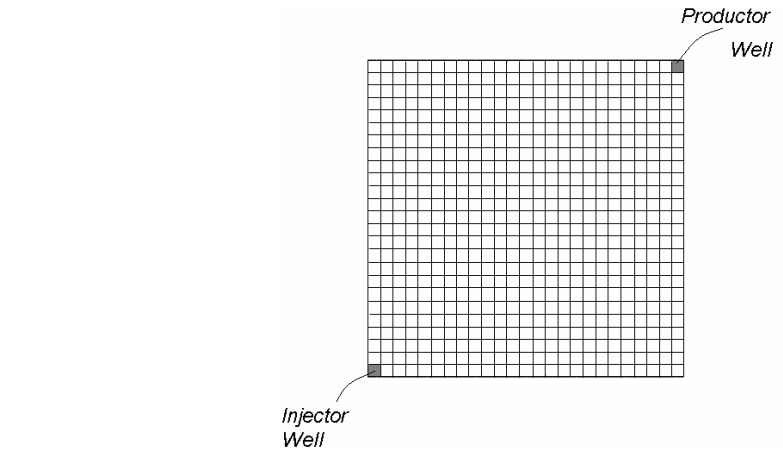

(a)

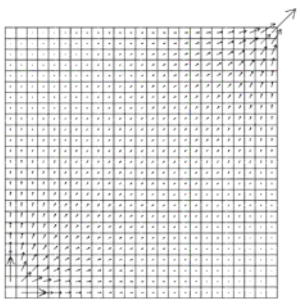

(b)

Fig. 9. *(a)* Typical "Five-Spot" configuration; *(b)* Field of groundwater velocities this configuration

Two situations are examined; the injection of the tracer during some specified time step and the continuous injection of the tracer. The results are compared with the data reported by Santos *et al*[21]. Table 1 gives the data used in the simulation and in the experimental work.

Tab. 1 Data used in the simulation and experiment

Parameter	Value
Dimension	**15 x 15 cm^2**
Permeability	**519 mDa**
Porosity	**0,1775**
Injected flow rate	**0,004116 cm^3/s**
Dispersion coefficient	**0,00115 m**

1 Darcy (Da) is equivalent to 0,987.10^{-8} cm^2

Fig.10 shows the tracer concentration at the production well for the two cases. The pulse injection of the tracer was equal to 0,4 porous volume (*PVI*). For definition, the porous volume injected is given by

$$PVI = \frac{W.t}{\mathcal{V}.n} \tag{30}$$

where W is the volumetric flow rate , t the injection time, V the volume, and n the porosity.

Fig. 10 shows the results of the pulse and of the continuous injection in a grid of 10x10 volumes and time step, Δt, equal to 2,77 h. The results can be considered very good, since the numerical method well captured the tracer fate in the production well. Moreover, the concentration peak of the pulse is also in a good agreement with the experimental data. Good results are also obtained for the continuous injection of the tracer, where it can be seen that the tracer concentration at the production well tends to unity for large time levels.

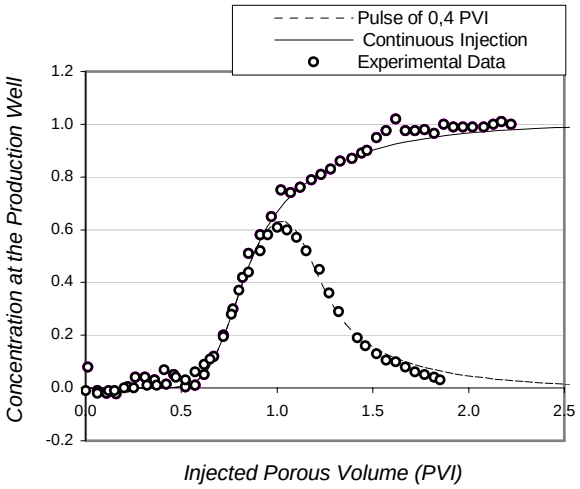

Fig. 10. Concentration at the production well. The solid and dotted curves represent the numerical results for continuous injection and a pulse of 0,4 *PVI* injection. The points are experimental data of Santos *et al*[20].

5.3. Simulation of a heterogeneous aquifer contamination

The next example is a groundwater contamination where the hydraulic permeability of the central region of the domain is close to zero. Therefore, the flow will tend to avoid this region. It is simulated a spill of gasoline with 30 kg of BTEX, in a area of 3 m^2 of an aquifer of fine clay with 1 m thickness and permeability of 5.10^{-18} m^2. The prescribed velocity is 0,9 m/day in the left face and zero derivative at the right face of the domain. The other faces are impermeable. The domain of 31x21 m^2 was discretized using a grid of 31x21 volumes. The retard factor is R = 1,2. The longitudinal dispersion is $\alpha_L = 0{,}26$ m and the transversal is $\alpha_T = 0{,}015$ m. The BTEX maximum solubility was assumed as 1 g/l. Fig. 11 depicts the boundary conditions and other details of the problem.

The flow solution is shown in the Fig.12, where the flow has the tendency to deviate from the low permeability region, as expected. The contaminant transport without decay was simulated for six distinct time levels: 10, 30, 50, 60, 70 e 75 days, using time step, Δt, equal to 0,1 day. Fig. 13 shows the iso-concentrations lines for several simulation times. It is clear that in the beginning of the simulation, until approximately 30 days, the low permeability region works as barrier, but not hindering the propagation of the contamination.

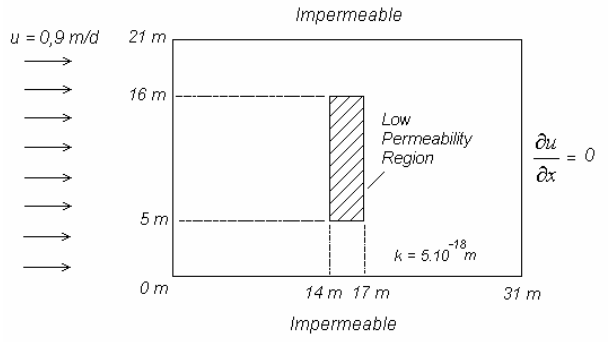

(a)

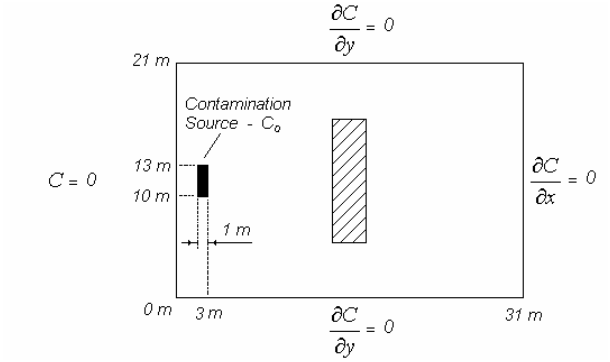

(b)

***Fig*. 11. *(a)* Flow boundary conditions, and *(b)* concentration boundary conditions of the heterogeneous aquifer contamination problem**

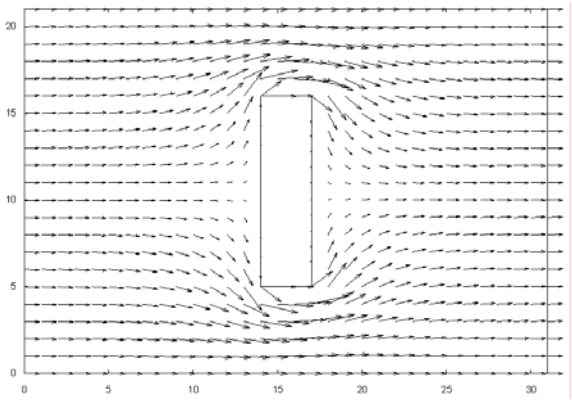

Fig. 12. Velocity vectors for the aquifer given in Fig. 11

5.4. Simulation of a one-dimensional contamination of ethanol-amended gasoline

As a final application, the contamination problem using the model with considers the presence of ethanol is solved. Results for the BTEX concentration are compared with the model with no ethanol in the gasoline. This case involves the spill of 100 liters of the Brazilian commercial gasoline, which is composed of 24 liters of alcohol and 76 liters of pure gasoline. As its volumetric fraction in the gasoline is 0,42 %, there is 0,32 liters of benzene. Its specific mass is 870 kg/m^3, therefore, 0,277 kg of this compound is present in the mixture. It is easy to show using Raoult's Law, that the maximum amount of benzene able to migrate to the aqueous solution is 18 mg/l. However, the presence of ethanol increases the benzene solubility, according to Eq. (2). The data needed to calculate the new benzene solubility are

- benzene solubility in the pure water S_w = 18 mg/l;
- the volume fraction of the ethanol in the gasoline f_c = 0,24;
- the relative increasing of solubility $\overline{\beta}$ = 0,665

Solving Eq. (2), the benzene solubility in the water/co-solvent mixture, S_m, increases to 26 mg/l. This value will be maintained as the prescribed concentration of the contamination while the contamination source has available mass to spill. When the ethanol is fully consumed, the benzene solubility in the source will return to the value 18 mg/l. Since the ethanol specific mass is 790 kg/l, there is 19 kg of ethanol that will fully dissolve in the groundwater, since the ethanol solubility in the water is assumed to be infinite.

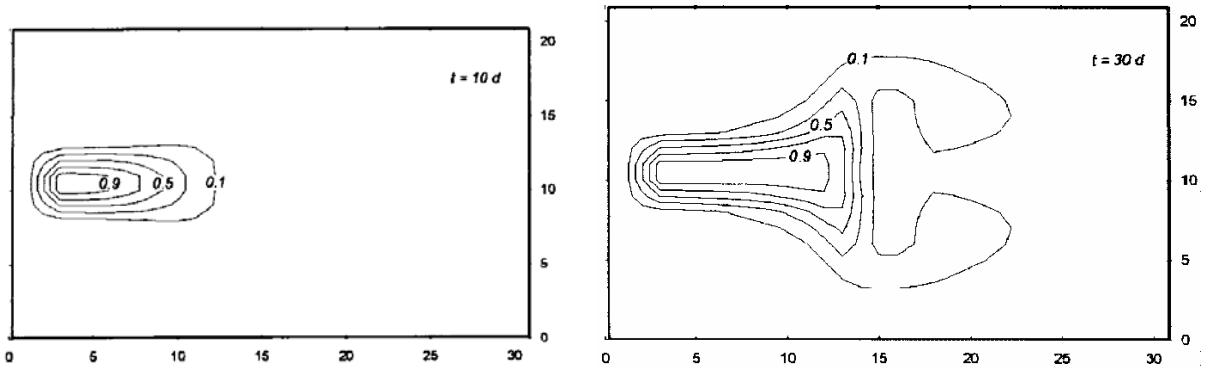

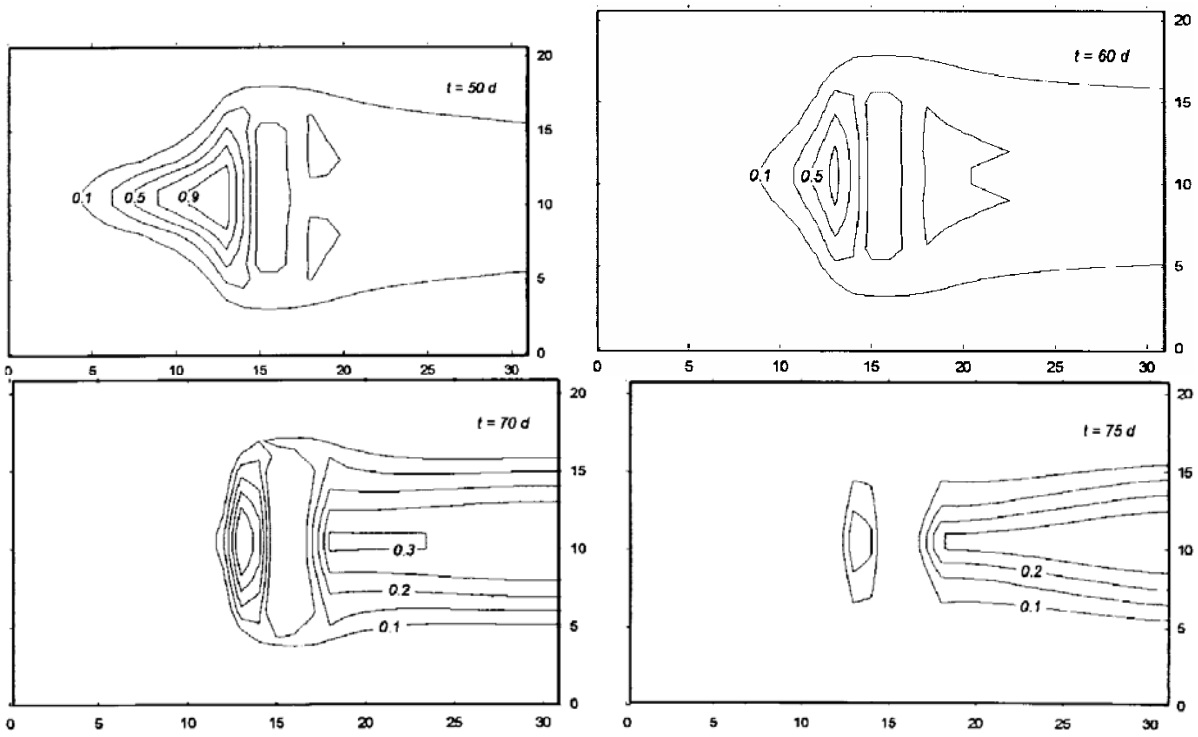

Fig. 13. Pollutant concentration for time levels of 10, 30, 50, 60, 70 e 75 days

The 1D solution domain is 30m long discretized with 40 volumes, as shown in Fig. 14. The contamination source is located at x = 1,125 m. The boundary conditions are $C(0,t) = 0$ with a locally parabolic condition in x = 30 m. The values adopted for the first order decay, λ, were 0.1 day^{-1} and 0.2 day^{-1}, for benzene and for ethanol, respectively. The plume retard factor, R, is assumed equal to 1.0 for the ethanol and 1.12 for the benzene. The groundwater velocity is 0.25 m/day and the longitudinal dispersion coefficient, α_L = 0,01 m. The minimum value of ethanol concentration able to retard the benzene biodegradation (that justifies the adoption the value δ =0 in the BTEX transport equation), is under investigation, but here it is assumed 3 mg/l.

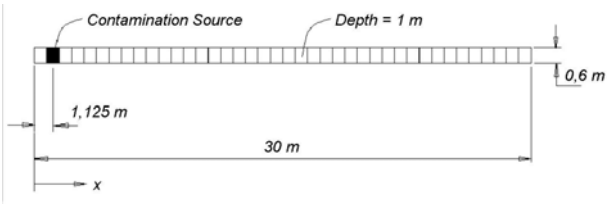

Fig. 14. Physical domain of the one dimensional problem of the benzene contamination amended-ethanol

Fig.15 presents the results of the simulation for the benzene concentration after 320 days. It is clear the influence of the ethanol in the benzene consumption by biodegradation. Without ethanol in the gasoline the benzene concentration peak is around 0.1, while with the presence of ethanol it reaches a peak four times greater.

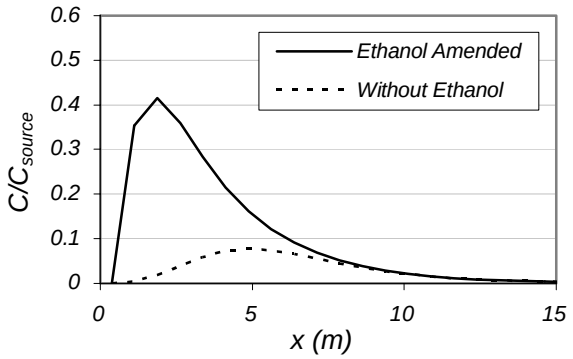

Fig. 15. Comparison of dimensionless benzene concentration after 320 days, as a function of the distance, with and without ethanol in the gasoline

6. CONCLUSIONS

The contamination with BTEX compounds, unfortunately, occurs very often and to predict the fate of these species is extremely important for safety and health reasons. It is a world tendency to add ethanol to the gasoline, in order to decrease the emission of toxic gases. However, the presence of ethanol in gasoline retards the heavy contaminants biodegradation, as could be seen in this work. The main contribution this work is to present an approach for modeling and simulating groundwater contamination. It is shown that it is possible to model the biodegradation with a first order decay for ethanol.

To model the increasing of the contaminant solubility in the aqueous phase in presence of ethanol (the co-solvency effect), it was assumed that the hydrophobic compounds solubility in water (BTEX, for example) increases log-linearly with the fully miscible organic solvents volume fraction. The inclusion of co-solvency phenomena in the model and the application of Raoult's Law in the definition of the dissolved mass of the source contamination can be considered as important contributions of this work.

The sorption effect was modeled by the Freundlich's isotherm, where the distribution coefficient b was assumed to be unity. This assumption simplifies the numerical scheme, since it avoids non-linearity in the model, but it is recommended in cases of low contaminant concentrations and low sorption potential. The numerical scheme developed can now be used to simulate different biodegradation models and, associated to experimental measurements, can be of extremely value in creating new biodegradation models.

Even though the authors had no enough field data to full validate physically the model, the results followed the physical trends and the numerical model developed can be very useful to help in predicting contaminant dispersion in groundwater flows.

7. REFERENCES

[1] Newell, C. J., Mcleod, R. K., Gonzalez, J. R., 1996, BIOSCREEN User's Manual. National Attenuation Decision Support System. *Version 1.3*, National Risk Management Research Laboratory, EPA/600/R-96/087, August.

[2] Domenico, P. A., 1987, An Analytical model for Multidimensional Transport of a Decaying Contaminant Species. Journal of Hydrology, 91, 49-58.

[3] Rifai, H. S., Newell, C. J., Gonzalez, J. R. Dendrou, S. Kennedy, L., Wilson, J. T., 1998, BIOPLUME III Natural Attenuation Decision Support System. National Risk Management Research Laboratory, EPA/600/R-98/010, January.

[4] Konikow, L. F., Bredehoeft, J. D., 1978, Computer Model of Two-Dimensional Solute Transport and Dispersion in Ground Water. Techniques of Water Resources Investigation of the United States Geological Survey, Book 7, Reston, VA.

[5] Fernandes, M., Corseuil, H. X., 1996, Groundwater Contamination by Gasoline Spill: Co-solvency Effect. In: 3º. Simpósio Ítalo-Brasileiro de Engenharia Sanitária e Ambiental (SIBESA), in Portuguese, Gramado, Junho.

[6] Santos, R. C. dos., 1996, The Influence of the Ethanol in the BTEX Biodegradation in groundwater contamination by Gasoline. *Master Thesis* (in Portuguese). Environmental Engineering Department Federal University of Santa Catarina, Florianopolis, Brazil.

[7] Corseuil, H. X., Fernandes, M., 1999, Co-Solvency Effect in Aquifers Contaminated with Ethanol-Amended Gasoline. In *Natural Attenuation of Chlorinated Petroleum Hydrocarbons an Other Organic Compounds*. Proceedings of the Fifth International In Situ an On-Site Bioremediation Symposium, San Diego, CA, April; Alleman, b. C., Leeson, A., Eds.; Battelle Press: Columbus, OH, 1999; pp. 135-140.

[8] Yalkowsky, S. H. and Roseman, T.,1981, Solubilization of Drugs by Cosolvents. Techniques of Solubilization of Drugs. Yalkowski, S. H., Ed. Marcel Dekker, Inc: New York, p. 91-134.

[9] Bedient, P. B., Rifai, H. S., Newell, C. J., 1994, Ground Water Contamination: Transport and Remediation. Prentice-Hall PTR, New Jersey.

[10] Howard, P. H., 1990, Handbook of Environmental Fate and Exposure Data for Organic Chemicals. Vol. I and II, Lewis Publishers, Inc, Chelsea, MI.

[11] Weber Jr, W. J., Mcginley, P. M., And Lynn, E. K., 1991, Sorption Phenomena in Subsurface Systems: Concepts, Models and Effects on Contaminant Fate and Transport. Water Res., Vol. 25, No. 5, pp. 499-528.

[12] Cordazzo, J. and Maliska, C.R., 2001. Internal Report. *Laboratory of Numerical Simulation*, SINMEC. Federal University of Santa Catarina.

[13] Raithby, G. D. and Torrance, K. E., 1974, Upstream-Weighted Differencing Schemes and Their Application to Elliptic Problems Involving Fluid Flow, Computers e Fluids, Vol. 2, pp. 191-206

[14] Bear, J., 1969, Flow through Porous Media, (R. J. M. De Wiest, ed.), pp. 109-199. Academic Press, New York.

[15] Cordazzo, J., 2000, Modeling and Numerical Simulation of Groundwater Contamination by Ethanol Amended Gasoline, *Master Thesis* (in Portuguese), Mechanical Engineering Department, Federal University of Santa Catarina, Florianopolis, SC, Brasil.

[16] Bejan, A., 1995, Convection Heat Transfer. John Wiley & Sons, New York.
Cordazzo, J., 2001. Internal Report. *Laboratory of Numerical Simulation*, SINMEC. Federal University of Santa Catarina.

[17] Maliska, C. R., 1981. A Solution Method for Three-Dimensional Parabolic Fluid Flow Problems in Nonorthogonal Coordinates, PhD. Thesis, University of Waterloo, Waterloo, Canada.

[18] Maliska, C. R., 1995, Heat Transfer and Computational Fluid Mechanics, (in portuguese), LTC – Livros Técnicos e Científicos S.A., Rio de Janeiro, Brasil

[19] Sudicky, E. A., 1985. A Collection of Analytical Solutions for Solute Transport in Porous and Fractured Porous Media, report, Inst. For Groundwater Res., University of Waterloo, Ont.

[20] Santos, R. L. A., Pedrosa Jr., O. A., and Correa, A. C. F., 1992. An Efficient Finite-Volume Approach for Modeling Miscible Displacement, II Latin-American Petroleum Engineering Conference, Caracas, Venezuela, March